Bull. Chem. Soc. Ethiop. **2025**, 39(6), 1119-1136.
DOI: https://dx.doi.org/10.4314/bcse.v39i6.8
© 2025 Chemical Society of Ethiopia and The Authors
ISSN 1011-3924
Printed in Ethiopia
Online ISSN 1726-801X

SYNTHESIS, SPECTROSCOPIC STUDIES AND EVALUATION OF BIOLOGICAL ACTIVITY OF SOME SUBSISTUDED 1,2,4-TRIAZOLES AND THEIR COMPLEXES WITH Co(II), Ni(II) AND Zn(II) IONS

Intisar A. Mohammed, Amaal Y. Al-Assafe* and Anwar A. Fathi

College of Education for Pure Science, Mosul University, 41001, Mosul, Iraq

(Received January 22, 2025; Revised February 24, 2025; Accepted February 26, 2025)

ABSTRACT. The present work describes the synthesis and characterization of new Schiff base of (E)-6-(4-(5-mercapto-4-((1-(4-methoxyphenyl)ethylidene)amino)-4H-1,2,4-triazol-3-yl)phenyl)-5H-pyrrolo[3,4-b]pyridine-5,7(6H)-dione(L_2) by condensation reaction of 6-(4-(4-amino-5-mercapto-4H-1,2,4-triazol-3-yl)phenyl)-5H-pyrrolo[3,4-b]pyridine-5,7(6H)-dione (5)(L_1) with p- methoxy benzaldehyde. Using a 1:2 (metal : ligand) ratio, the ligands L_1 and L_2 were utilized to create a novel complex containing cobalt(II), nickel(II), and zinc(II) metal ions . Fourier transform infrared (FT-IR), ultraviolet-visible (UV-Visible), nuclear magnetic resonance (^{1}H-NMR, ^{13}C-NMR), micro elemental analysis (CHNS), thermal analysis, atomic absorption, molar conductance , and magnetic moment measurements have been used to examine and confirm new ligands (L_1, L_2) and their complexes. The observed data indicated the octahedral geometry around the Co(II), Ni(II)and Zn(II) complexes. Furthermore, the biological activity of ligands and its metal complexes in DMSO as control have also studied against four types of bacteria. The obtained results from inhibition zone values investigated that most metal complexes exhibited greater inhibition against all kinds of bacteria zone.

KEY WORDS: Triazole ligand, Transition metals, Benzohydrazide, 1,2,4-triazole complexes, Microbial activity

INTRODUCTION

In the past ten years, the 1,2,4-triazole moiety and its derivatives have garnered a lot of attention owing to their special properties[1]. It is simple to synthesize the triazole ring. Furthermore, a lot of these functionalized compounds are readily available, making them excellent, versatile, and rich in coordination chemistry. The π-conjugated complexes found in triazole rings can easily coordinate with metal ions and display phosphorescent characteristics. They contain nitrogen atoms as aromatic systems and hydrogen bond acceptors that match π–π bonding [2]. The 1,2,4-triazole moiety in a five-membered aromatic ring has three nitrogen atoms, with two atoms next to each other for stability, enhancing the water solubility. It can obtain 1H-isomer 1 and 4H-isomer 2, two isomers of tautomerism (Figure 1a). DFT and an empirical investigation both indicated that the 1H-tautomer is the preferable and more stable structure. Both nitrogen and carbon are attached to the carbon atom. 1,2,4-triazoles, results in an electron deficit in the triazole ring. As demonstrated, the triazole ring exhibits no electrophilic interaction. The molecule is not sensitive to typical carbon processes in aromatic chemistry, such as nitration. Notwithstanding the fact that the literature frequently discusses electrophilic attaks on the nitrogen atom [3-5]. The review of the literature showed that 1,2,4-triazole compounds have a broad range of bioactivities, such as antibacterial, anticancer, and anti-inflammatory characteristics. Analgesics, insecticides, antivirals, antidepressants, and microbes that regulate plant growth [6-9]. The biological activity of 1,2,4-triazole derivatives, which include the -SH group, makes them one of the most intriguing molecules among their subclasses [9-10]. It was revealed that most drugs and natural substances have mercapto-1,2,4-triazole as their primary ingredient (Figure 1b).

*Corresponding authors. E-mail: amaalyounis62@uomosul.edu.iq
This work is licensed under the Creative Commons Attribution 4.0 International License

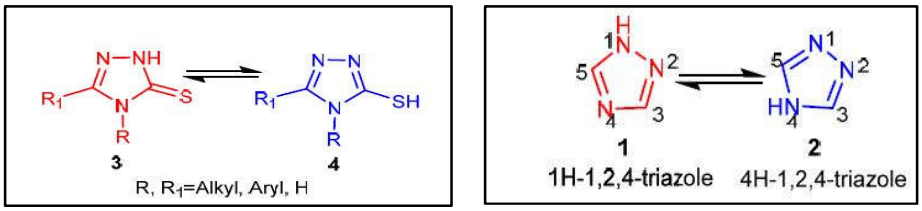

Figure 1. a. 1H- and 4H- 1,2,4-triazole tautomerism. b. Thione -thiol tautomeric forms.

Triazole derivatives' active sites have greatly aided researchers in creating metal complexes with these kinds of ligands [11-13]. Kanagarajan *et al.* [14] discovered two physiologically active Schiff base ligands prepared from 1,2,4-triazole by using thiophene-2-carbaldehyde and furan-2-carbaldehyde in the equimolar synthesis of 4-amino-5-(pyridin-4-yl)4H-1,2,4-triazole-3-thiol; their metal complexes of Co(II), Ni(II), and Cu(II) were characterized by spectroscopy. It has been shown that chelates of Pt(II), Pd(II), Ni(II), Co(II), and Sn(IV) with 4,5-diphenyl-1,2,4-triazole-3-thione as the primary ligand and 1,2-bis(diphenylphosphino) ethane as the secondary ligand exhibit anti-proliferative reactivity against various kinds of cancer cells.

The coordination compounds exhibited significant anticancer activity. The use of 1,2,4-triazoles to connect ligands between transition metal ions has been investigated. Generating coordination ligands containing 1,2,4-triazole moieties has received much attention recently. This is especially true for those that are formed of S and N atoms because of their biological properties in comparison with free ligands. [15, 16]. Some known complexes include 1,2,4-triazole moieties having two coordination sites with metal ions, such as S and N atoms. Therefore, in this study, 1,2,4-triazole derivatives ((L_1, L_2)were used to synthesize some metal complexes of Co(II), Ni(II), and Zn(II) ions.(L_1, L_2) acting as bi-dentate ligands to create novel complexes, followed by a study of the antibacterial activity of the ligands' and their metal complexes'.

EXPERIMENTAL

Materials

All substances and solvents were provided without further purification. Sigma-Aldrich provided the metal salts $CoCl_2.6H_2O$, $NiCl_2.6H_2O$, $ZnCl_2$, and pyridine 2,3-di carboxylic acid. The Fluka Company supplied hydrazine hydrate, *p*-methoxy benzaldehyde, CS_2, ethanol, DMF, and DMSO.

Instrumentation

FT-IR spectra (υ max (cm^{-1})) were measured using Shimadzu FT-IR84005 Spectrophotometer, Japan, between the ranges (200- 4000 cm^{-1}) as cesium iodide discs at Education for Pure Sciences College, Tikrit University. The ^{1}H-NMR and C^{13}-NMR tests were carried out at Sciences College, Basra University using Bruker-DRX system at 400 MHz, (TMS) as standard in DMSO-d_6. Electronic spectra measurements for ligands and their compounds at concentration(10^{-3} M) using DMF as a solvent at 25 °C were conducted utilizing the Shimadzu UV-Vis spectrophotometer Ultra Violet-1800Spectrophotometer at 190−1100 nm in Education for Pure Science College Mosul University. Element microanalyses were performed using a Leco 932 USA Elemental Analyzer (C.H.N). The molar conductance of the synthesized compounds was measured using the HANNA EC214conductivity meter in dimethylformamide at 25 °C in Education for Pure Science College, Mosul University. Metal ion analyses had been evaluated spectrophotometrically utilizing atomic absorption spectroscopy, Analytic Jena GmbH-novAA350 novAA350 at the

College of Agriculture and Forestry, University of Mosul. Sherwood Scientific was used to assess the produced complexes' magnetic susceptibility at room temperature (MSB-MK) at Education for Pure Sciences College, Tikrit University.

Synthesis of ligands (L_1, L_2)

*Synthesis of Furo [3,4-b] pyridine-5,7-dione (**1**)*

This compound was prepared by dissolving (0.02 mol, 6.3 g) of pyridine 2,3-dicarboxylic acid in acetic anhydride and then had been refluxed for an hour. After the reaction had finished as checked by TLC. The product solution cooled, the resulted precipitation was filtered, dried and recrystallized from ethanol to give yellow solid powder 77% (m p. 135 °C) [17].

*Synthesis of [4-(5,7-dioxo-5,7-hydro-6H-pyrrolo [3,4-b] pyridine-6-yl] benzoic acid (**2**)*

Compound **1** (0.02 mol, 3 g) was refluxed with (0.02 mol, 2.8 g) of 4-aminobenzoic acid, and 30 mL of acetic acid for an hour. The product evaporated then cooled and precipitated by ethyl acetate. The formed precipitate was filtered and recrystallized using acetic acid to obtain white powder in % 87 m.p. 307-309 °C.

*Synthesis of 6-(4-propionyl phenyl-5H-pyrrolo[3,4-b]pyridine-5,7- (6H)-dione] (**3**)*

The solution of concentrated sulfuric acid (3-5 mL) was added after compound **2** (0.02 mol, 5.36 g) had been dissolved in absolute ethanol. The reaction mixture had been refluxed for 6 h. After completion of the reaction was checked by TLC, followed by pouring the product into ice-cold water with stirring, 10% sodium bicarbonate was added to the solution until litmus paper turned blue. The ester layer was separated and extracting by using 20 mL water, ether layer was separated, dried using anhydrous $MgSO_4$. The obtained precipitate was filtered, dried, and recrystallized from ethanol to give brown solid powder in 79% m.p. = 295-297 °C.

*Synthesis of 4-(5,7-dioxo-5,7-dihydro-6H-pyrrolo[3,4-b]pyridin-6-yl)benzohydrazide (**4**)*

Compound **3** (0.02 mol, 3 mL) and hydrazine hydrate (0.02 mol, 3 mL) were dissolved in 30 mL ethanol and then refluxed for 5 h. The precipitate was filtered and recrystallized using ethanol (Figure 2). This compound resulted in a 80% yield as a white powder (m.p. 257 °C). IR, cm^{-1}) 3275, 3394 cm^{-1} (υNHNH₂), 1720, 1658, 1643, 1307 cm^{-1}, (asym. υC=O imide, υC=O amide, υC=C aromatic, and υC–N imide) [18, 19].

*Synthesis of 6-(4-(4-amino-5-mercapto-4H-1,2,4-triazol-3-yl)phenyl)-5H-pyrrolo[3,4-b]pyridine-5,7(6H)-dione (**5**)(L_1)*

To a potassium hydroxide solution in absolute ethanol, benzohydrazide (**4**) (0.003 mol, 1 g) and carbon disulfide (0.006 mol, 0.45 mL) were added and the mixture was stirred for 12 h. After filtering, ether washing, and vacuum drying, the precipitate was utilized in the following step. The generated potassium salt hydrazine hydrate (1.5 mL) in (1 mL) water was refluxed for 5 h. By diluting the solution with 25 mL of water and acidifying it with acetic acid, it yielded a white precipitate that was filtered, dried, and recrystallized from DMF (Figure 2), m.p. 315-317 °C. Yield % 72). IR, cm^{-1} 3311, 3193, 2760, 1683, 1301, 634); CHNS elemental analysis calculated for ($C_{15}H_{10}N_6O_2S$): C, 53.25%; H, 2.98%; N, 24.84%; O, 9.4 6%.; S% 9.48. Found: C, 52.88; H, 2.95; N, 24.61; O, 9.24; S% 9.34). ^{1}H NMR (400 MHz, DMSO-d_6, δ ppm): 13.32 (s, weak, SH),

7.30-8.20 (7H, aromatic ring), 4.87 (S, broad, NH_2); ^{13}C-NMR 174, 154, 145 (C=S thione), (–C=N–triazole ring), 120–124 ppm (aromatic carbon atoms) [19].

*Synthesis of (E)-6-(4-(5-mercapto-4-((1-(4-methoxyphenyl)ethylidene)amino)-4H-1,2,4-triazol-3-yl)phenyl)-5H-pyrrolo[3,4-b]pyridine-5,7(6H)-dione (**6**)(L_2)*

Ligand (L_1) (0.001 mol, 0.336 g) and *p*-methoxy benzaldehyde (0.001 mol, 4 mL) in absolute ethanol with two or three drops of glacial acetic acid were refluxed for 4 h with stirring, evaporated the solvent, then washed with ether, dried, and recrystallized from ethanol (Figure 2). Yield % 89 m.p. L2 = 170-172 ºC as a yellow powder. IR, cm^{-1} 1658 (CH=N), 2621 (SH), 1254 C=S, 615 (C-S) (Figure 3b). CHNS calculated for $C_{23}H_{16}N_6O_3S$ (L_2): C, 60.52%; H, 3.57%; N, 18.51%; O, 10.51%.; S% 7.04. Found: C, 60.47; H, 3.52; N, 18.36; O, 10.48; S% 7.01. ^{1}H NMR in DMSO-d_6; δ = 9.02 ppm (N=CH) showed a signal at δ = 3.81 (methoxy group), 4.02 ppm (phenolic proton), δ = 6.2-8.06 protons aromatic, 8.6 ppm (triazole ring) spectra showed a signal at δ = 13.77 ppm (S-H). The ^{13}C-NMR δ = 118 ppm (four unsubstituted aromatic cyclic carbons), δ =122 ppm (carbon atom of phenyl linked to the triazole group), multiple band at δ = 133-137 (N=CH) ppm, δ =162-165 ppm (carbon atom attached to the SH(C=S) group in the triazole ring) [20].

*General procedure of preparation of complexes in a ratio of (2:1 (L:M) (**7**-**12**)*

In 100 mL round bottom flask 0.001 mol of the prepared ligands (**1**, **2**) was dissolved in 15 mL absolute ethanol and added to it a solution consisting of dissolving (0.001 mol) of the metal salt ($CoCl_2.6H_2O$) or ($NiCl_2.6H_2O$) or ($ZnCl_2$) in 5 mL absolute ethanol and added (0.001 mol, 0.14 mL) to the mixture of triethylamine dissolved in 5 mL absolute ethanol. The mixture was heated with stirring for 2 h. The resulted solution was cooled, and the resulting precipitate was filtered and recrystallized from ethanol [10, 21]

*Complex (**7**).* It was prepared from ligand (**1**) with ($CoCl_2.6H_2O$) and resulted in 60% as a reddish brown powder (m.p. 288^d ºC). IR cm^{-1} 3240, 3082 (NH_2asy, sym), 1186 (C=S), 696 (C-S) and 1643 (C=Nof triazole ring), 555 (Co-N), 384 (Co-S), 227 (Co-Cl). CHNS calculated for $C_{30}H_{20}Cl_2N_{12}O_4S_2Co$: C, 44.68%; H, 2.50%; N, 20.84%; Cl, 8.79%; O, 7.93%; Co, 7.31. Found: C, 43.50%; H, 2.45%; N, 19.77%; O, 7.22%; Co, 7.11.

*Complex (**8**)*. It was prepared from ligand (**1**) with ($NiCl_2.6H_2O$) and resulted in 65% as a light green powder (m.p. 286^d ºC). IR cm^{-1} 3250, 3080 (NH_2asy, sym), 1645 (C=N), 1180 (C=S), 687 (C-S), 551 (Ni-N), 366 (Ni-S), 233 (Ni-Cl). CHNS calculated for $C_{30}H_{20}Cl_2N_{12}O_4S_2Ni$: C, 44.68%; H, 2.50%; N, 20.84%; Cl, 8.79%; O, 7.93%; Ni, 7.88. Found: C, 43.50%; H, 2.45%; N, 19.77%; O, 7.22%; Ni, 9.20.

*Complex (**9**)*. It was prepared from ligand (**1**) with ($ZnCl_2$) and result in 61% as a light yellow powder (m.p. 292^d ºC). IR cm^{-1}, 3260, 3090 (NH_2asy, sym), 1655 (C=N), 1187 (C=S), 690 (C-S), 511 (Zn-N) and 356 (Zn-S), 298 (Zn-Cl). CHNS calculated for $C_{30}H_{20}Cl_2N_{12}O_4S_2$ Zn: C, 44.32%; H, 2.48%; N, 20.68%; Cl, 8.72%; O, 7.87%; S, 7.89. Found: C, 44.98%; H, 2.21%; N, 19.88%; Cl, 8.20%; O, 7.41%; S, 7.53.

*Complex (**10**)*. It was prepared from ligand (**2**) with ($CoCl_2.6H_2O$) and result in 71% as a violet green powder (m.p. > 300^d ºC). IR cm^{-1} 1607 (C=N), 1242 (C=S), 520 (Co-N), 375 (Co-S), 233 (Co-Cl). CHNS calculated for $C_{49}H_{39}Cl_2N_{12}O_6S_2Co$: C, 54.20%; H, 3.62%; N, 15.48%; Cl, 6.53%; O, 8.84; Co, 5.43. Found: C, 53.70%; H, 3.11%; N, 14.88%; Co, 4.88.

Complex (11). It was prepared from ligand (**2**) with ($NiCl_2.6H_2O$) and result in 74% as a green powder (m.p. > 300^d ºC). IR cm^{-1} 1604 (C=N), 1245 (C=S), 520 (Ni-N), 380 (Ni-S), 232 (Ni-Cl). CHNS calculated for $C_{49}H_{39}Cl_2N_{12}O_6S_2Ni$: C, 54.20%; H, 3.62%; N, 15.48%; Cl, 6.53%; O, 8.84; Ni, 5.53. Found: C, 53.80%; H, 3.12%; N, 13.24%; Ni, 5.42.

Complex (12). It was prepared from ligand (**2**) with ($ZnCl_2$) and result in 76% as a lemon yellow powder (m.p. > 300^d ºC). IR cm^{-1} 1606 (C=N), 1246 (C=S), 518 (Zn-N), 374 (Zn-S), 287 (Zn-Cl). CHNS calculated for $C_{49}H_{39}Cl_2N_{12}O_6S_2Zn$: C, 53.88%; H, 3.60%; N, 15.39%; Cl, 6.49%; O, 8.79; S, 5.87. Found: C, 52.99%; H, 3.13%; N, 14.29%; Cl, 5.72%; S, 5.78.

Biological study

The biological impact of several prepared compounds (L_1, L_2, **3**, **4**, **5**, **6**) has been studied against four types of bacteria, both Gram-positive and Gram-negative bacteria; these bacteria are *Staphylococcus aureus*, *Escherichia coli*, *Klebsiella pneumonia*, and *Salmonella typhi*, obtained from the laboratories of the Department of Life Sciences, College of Pure Science, University of Mosul.

Inhibition activity test the Levne method [22], which is based on the Vandepitte method [23], was followed. Nutrient saline medium was injected with individual colonies of the mentioned bacteria separately. The bacteria were then incubated at a temperature of 37 ºC for 18-24 h. Subsequently, a series of dilutions were made with normal saline solution to obtain a concentration equivalent to 108 cells/cm^3, compared to tube number 1 of Macfarland standard tubes. To study the antibacterial effect of the prepared compounds, filter paper discs with a diameter of 6 mm were saturated with specific concentrations of the compounds dissolved in DMSO, which were selected. Then, the discs were placed on the surface of agar plates using sterilized forceps and incubated at a temperature of 37 ºC for 18-24 h afterward, the inhibition zone diameter was measured and compared to some plates with standard antibiotics (tetracycline) as standard samples.

RESULTS AND DISCUSSION

The new Schiff base L_2 was synthesized using the synthetic approach shown in Figure 2. The ester (**3**) was formed by heating compound (**2**), and substituted benzoic acid, in ethanol with a catalytic quantity of concentrated H_2SO_4. The reaction of compound (**3**) with hydrazine hydrate in ethanol produced benzohydrazide (**4**).

When compound (**4**)was treated with carbon disulfide and alcoholic potassium hydroxide, excess hydrazine hydrate in ethanol yielded L_1 (**5**). Condensation of L_1 (**5**) with *p*-methoxy benzaldehyde in refluxing ethanol gave L_2 (**6**). The ligands (L_1, L_2) and their metal complexes were subjected to elemental analyses. The results obtained are in good agreement with those calculated for the suggested formula. The structures of the synthesized ligands and their metal complexes are also confirmed by IR, UV-Visible, ^{1}H-NMR, and ^{13}C-NMR spectral analysis, magnetic susceptibility, molar electrical conductivity, and thermal analysis (TGA, DTA), which are discussed below. The data reveal that the complexes of synthesized metals (II) are air-stable, microcrystalline solids, insoluble in common organic solvents, but all are soluble in DMF and DMSO, and the ligand was used as a bi dentate ligand (Lewis base) to prepare metal complexes through the reaction of ratio (1:2) metal:ligand.

FT-IR spectral study

The synthetic compounds have been characterized by assigning stretching vibration bands using the infrared spectrophotometer technique. The FTIR spectrum of L_1 (Figure 3a) shows some characteristic stretching bands at 3311, 3193, 2760, 1683, and 634 cm^{-1}, allocated to NH_2 (asym,

sym), S-H, and C=N of the triazole ring, while the last one is for the C-S bond's stretching [24] (Figure 3a). Complexes **7-9** showed a change in the positions and intensities of the bands, as shown in (Figure 3c). Therefore, the thiol group (S-H) in L1 disappears after coordination due to the tautomeric form, which can occur in the triazole ring. Therefore, the thiol functional group (S-H) in the ligand molecule disappears after complexation due to the tautomer form, which can occur in the triazole ring (Figure 1) [25].

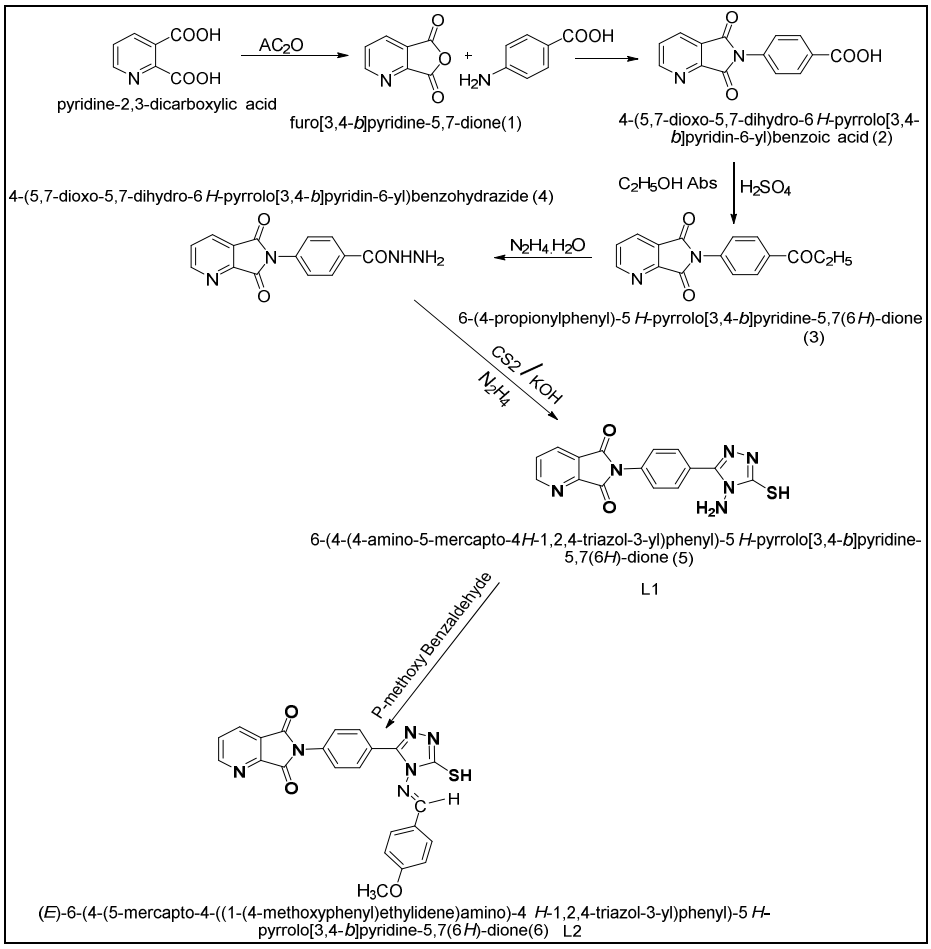

Figure 2. Synthesis of L_1, L_2.

Compared to the ligand L_1, the υ(C=N) and υNH_2 (asym and sym) bands of complexes **7-9** had been changed to a lower wavelength number, suggesting the coordination occurred through the nitrogen atom of amine group [26]. When the complexes were formed, the υ(S–H) band disappeared, and the υ(C=S) band also shifted to a higher or lower frequency due to the increase in the order of the C=S bond resulting from the coordination of the metal ion to the ligand through the sulfur atom. The appearance of new bands υ(M-N), υ(M-S), and υ(M-Cl) in the range 200-500 cm^{-1} confirms the occurrence of coordination and formation of complexes [27-30].

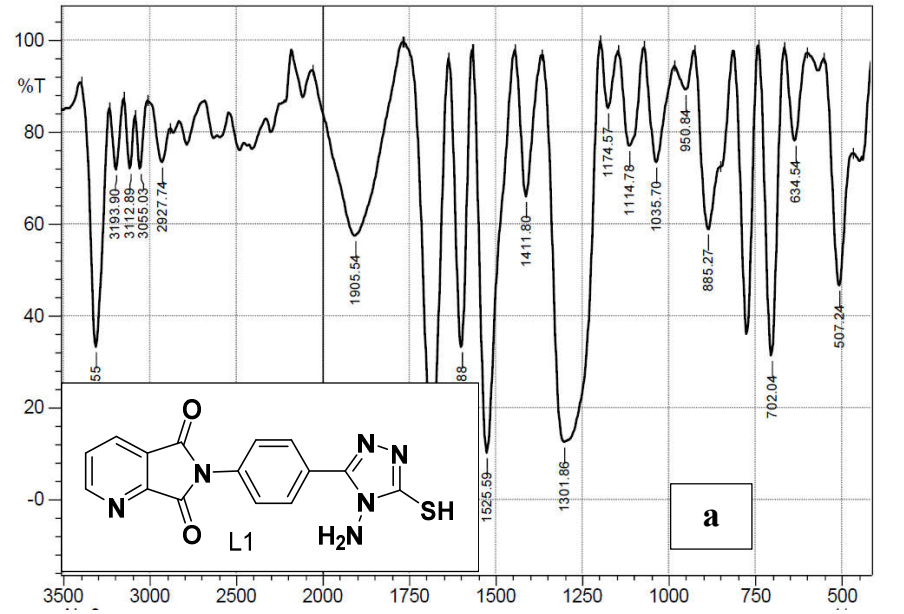
100
%T
80
60
40
20
-0
3193.90
3112.89
3055.03
2927.74
1905.54
1525.59
1411.80
1301.86
1174.57
1114.78
1035.70
950.84
885.27
702.04
634.54
507.24
3500
3000
2500
2000
1750
1500
1250
1000
750
500
O
N
O
N
N
N
N
SH
H2N
L1
a

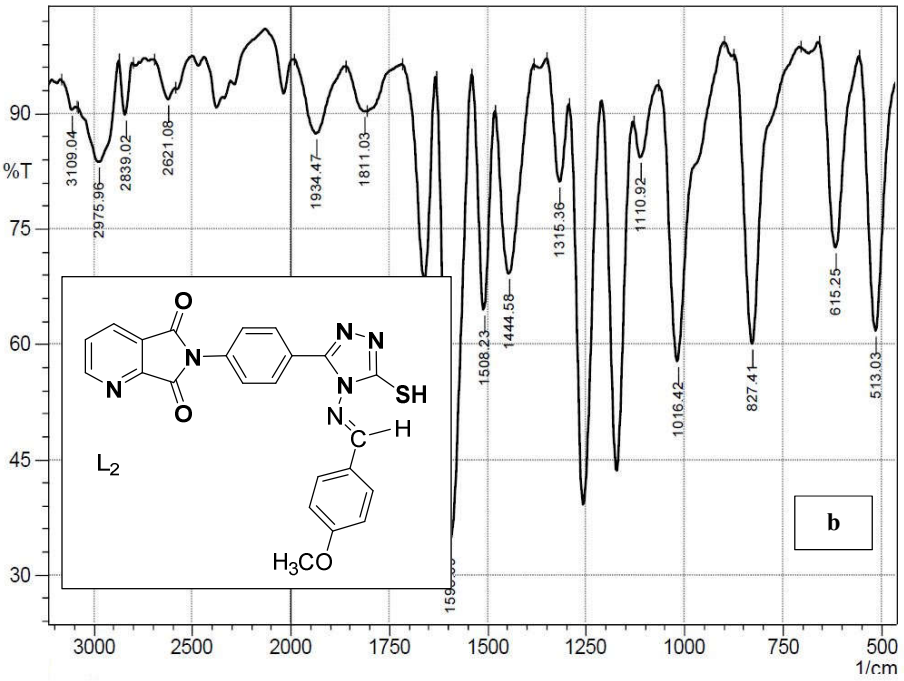
90
%T
75
60
45
30
3109.04
2975.96
2839.02
2621.08
1934.47
1811.03
1508.23
1444.58
1315.36
1110.92
1016.42
827.41
615.25
513.03
3000
2500
2000
1750
1500
1250
1000
750
500
1/cm
O
N
O
N
N
N
SH
N
C
H
L2
H3CO
b

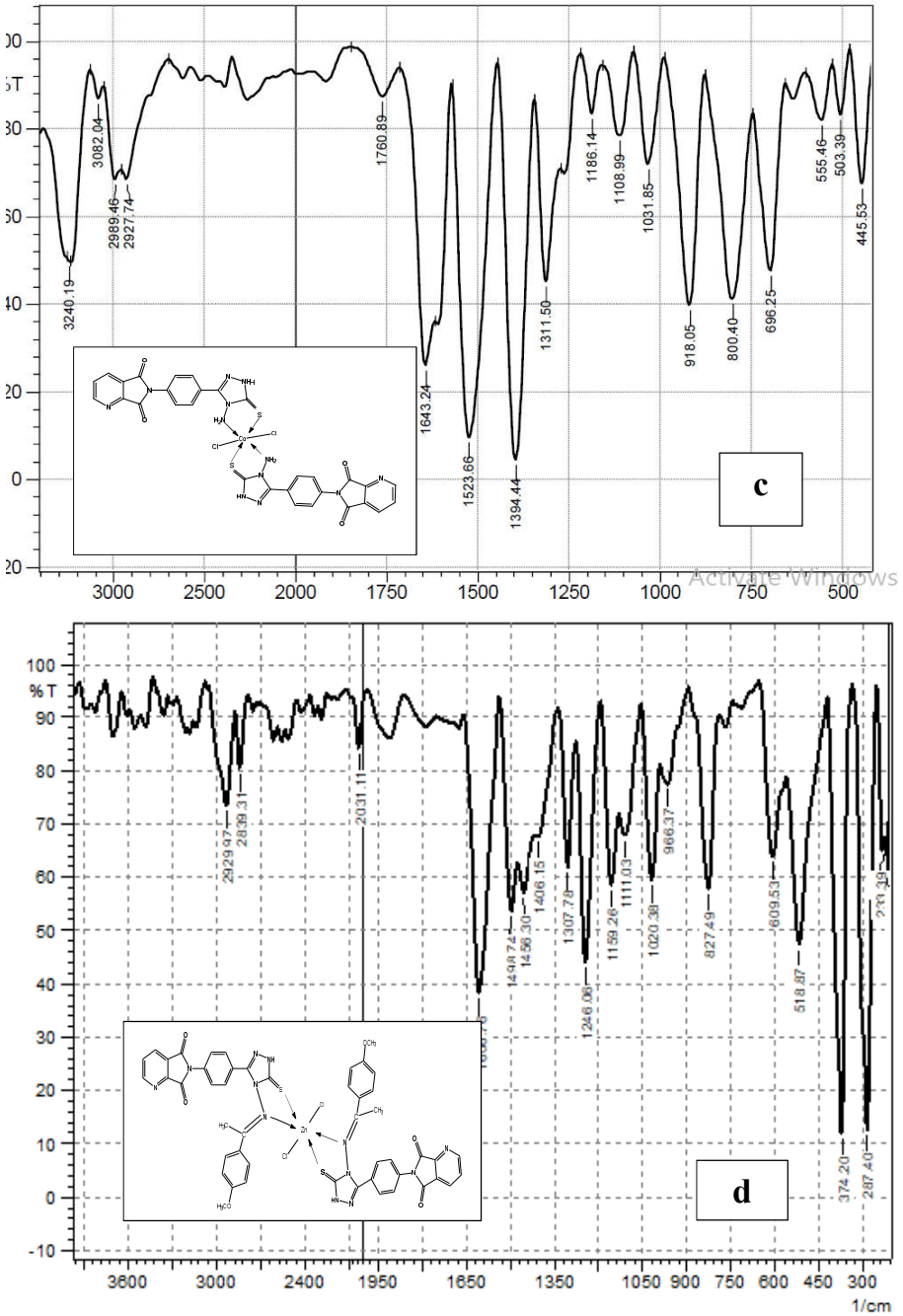

Figure 3.Infrared spectra of a: L_1, b: L_2 , c: $[Co(L_1)Cl_2]$,d:$[Zn(L_2)Cl_2]$.

The FTIR spectra of the ligand (L_2) (Figure 3b) showed various alterations. The disappearance of a band at 3311 and 3193 cm^{-1} was due to the stretch of υ(NH_2) (asym and sym), and the appearance of a new set of sharp stretching vibration bands at the frequency that is identical to the υ(C=N) imine group confirmed the formation of the Schiff base at 1658 cm^{-1}, and υ(S–H) appeared as a weak band at 2621 cm^{-1}. In the spectra of prepared complexes (Figure 3d), the (C=N) imine group in the ligand (L_2) was moved to a lower wavenumber, indicating that the (C=N) imine group was coordinated with the metal via the N atom. However, the (C=S) stretching vibration shifted to higher frequencies or appeared as multiple bands with different shapes and reduced intensity. The IR spectra revealed that the Schiff base (L_2) acts as a bi-dentate ligand via the nitrogen of the azomethine group (CH=N) and sulfur of the thione group(C=S). However, the novel weak bands at υ(232-518) cm^{-1} are associated with υ(M-N), υ(M-S) and υ(M-Cl) coordination bonds [31].

NMR spectra studies

The ^{1}H-NMR (400 MHz, $CDCl_3$, δ ppm) spectrum of compound (L_1) showed four singlet peaks: at δ = 4.87 (s, broad, NH_2), at δ = 13.32 ppm (s, weak, SH), and at 7.30-8. 20 (7H aromatic) and at δ = 8.59 ppm (s,N-H of the triazole ring).

The ^{13}C-NMR spectra exhibited signals at 120–124 ppm (aromatic carbon atoms of triazole ring) at 167, 154, and 145 ppm that corresponded to the –C=S thione moiety.

Furthermore, the Schiff base ligand (L_2) was characterized using ^{1}H-NMR and ^{13}C-NMR. A singlet signal 8.5 ppm (1H) was observed corresponding to the Schiff base proton (CH=N). The chemical shifts of aromatic, triazole ring, and thiol protons appeared at 6.2–8.06 and 13.12 ppm, respectively [32].

An important characteristic of the ^{13}C-NMR spectra of L2 was the presence of signals of the azomethine group (N=CH) at 163 ppm and aromatic carbons at 113 to 132 ppm [33, 34].

Magnetic measurements and electronic spectra

The prepared cobalt(II) complexes that possess the cobalt(II) system (d^7) has three unpaired electrons gave the electronic arrangement t_2g^5 eg^2 and have magnetic moment values ranging between (4.56-4.96) B.M. (Table 1).

The effective magnetic moment value is higher than the theoretically calculated value, which indicates the presence of the orbital contribution, and this is consistent with the values of the magnetic moment for the hexagonal cobalt(II) complexes with a highly twisted octahedral geometric shape [35, 36].

The electronic spectra of cobalt(II) complexes (Table 1) showed that the complexes (**7**, **10**) show three bands: the first band is υ_1 located in the range υ_1 (13660-13673) cm^{-1}, the second band υ_2 is in the range 17999-19012 cm^{-1}, and the third band υ_3 (29119-29475) cm^{-1} of the spectrum, in addition to the charge transfer band, which appears above cm^{-1} (30000) (Table 1). The appearance of bands υ_1, υ_2, and υ_3 confirms that these transitions are permissible. It goes back to octahedral cobalt complexes [29].

In comparing the μ_{eff} and μ_{obs} values for nickel(II) complexes, it is found that the μ_{obs} values are higher than the μ_{eff} values. The μ_{obs} value lies in the range of 4.71-4.73 B.M. This could be attributed to the following factors: The spin-orbit coupling is higher for $(t_2g)^6$ $(eg)^2$ configurations due to the positive quantity of α, Δ, and the negative quantity of λ. This leads to the orbital angular momentum being quenched. The observed magnetic moment is therefore higher than the calculated value.

In the present investigation, three absorption bands observed for the nickel(II) complexes **8**, **11** (Table1) are in general assigned to the following three transitions: the first band is υ_1 located in the range υ_1 (13730-14728) cm^{-1}, the second band υ_2 is in the range 18421-18425 cm^{-1}, and the

third band υ_3 (29470-29472) cm^{-1} of the spectrum, in addition to the charge transfer band, which appears above cm^{-1} (30000). The electronic spectra and magnetic moments of Co(II) and Ni(II) complexes suggest that are spin free and therefore octahedral geometry[37-38]

The electronic spectra of zinc(II) complexes did not show an absorption band for the (d-d) transition because the d orbital is a field (d^{10}-system). The charge transfer between Zn(II) and the ligand caused a change in the band position in comparison to the free ligand [39] listed in Table 1.

Table 1. Magnetic properties and electronic spectral data on metal complexes in DMSO (10^{-3} M).

Comp. No.	Comp. symbol	$\nu_1(cm^{-1})$	$\nu_2(cm^{-1})$	$\nu_3(cm^{-1})$	C.T. (cm^{-1})	µeff B.M.	Suggested structure
7	$[Co(L_1)_2Cl_2]$	13673 $^4T_1g(F)\rightarrow {}^4T_2g(F)$	17990 $^4T_1g(F) \rightarrow {}^4A_2g(F)$	29475 $^4T_1g(F)\rightarrow {}^4T_1g(P)$	35055	4. 96	Oh
8	$[Ni(L_1)_2Cl_2]$	14728 $^3A_2g \rightarrow {}^3T_1g(P)$	18421 $^3A_2g \rightarrow {}^3T_1g(F)$	29470 $^3A_2g \rightarrow {}^3T_2g(F)$	35037	4.73	Oh
9	$[Zn(L_1)_2Cl_2]$	-------	-------	-------	34981	-------	Oh
10	$[Co(L_2)_2Cl_2]$	13660 $^4T_1g(F)\rightarrow {}^4T_2g(F)$	19012 $^4T_1g(F) \rightarrow {}^4A_2g(F)$	29119 $^4T_1g(F)\rightarrow {}^4T_1g(P)$	34661	4.56	Oh
11	$[Ni(L_2)_2Cl_2]$	13730 $^3A_2g \rightarrow {}^3T_1g(P)$	18425 $^3A_2g \rightarrow {}^3T_1g(F)$	29472 $^3A_2g \rightarrow {}^3T_2g(F)$	34891	4.71	Oh
12	$[Zn(L_2)_2Cl_2]$	------	-------	-------	34775	------	Oh

The molar conductance of the prepared compounds was measured at a concentration of 10^{-3} M using the solvent dimethyl sulfoxide (DMSO), and the values ranged between 12-30 $cm^2.ohm^{-1}.mol^{-1}$. It was found from the molar electrical conductivity measurements that it agrees with the proposed structural formulas for the prepared complexes of the type (1:2) and falls within the range of complexes with neutral behavior, non –electrolytes, or weak conductors [40].

Differential and gravimetric thermal analysis of complexes

We observe from the results of the thermogravimetric analysis (TGA) measurement of the complex $[Co(L_1)Cl_2]$ that there are three main changes. The first change begins at (160-180 ºC), which has been attributed to the loss of CO_2 as a result of the carbonyl group dissociation at this range, and its percentage was 30%. The second is within the temperature range (380-430 ºC), which is attributed to the beginning of ligand decomposition with a weight loss of approximately (20%). The third decomposition, which falls within the range (440-520 ºC), is due to the complete ligand decomposition, resulting in a total weight loss of around 20%. It's worth noting that these changes match and align with differential thermal analysis (DTA) (Figure 4). Thermogravimetric analysis of the complex $[Ni(L_2)Cl_2]$ was also studied, as we notice through the thermogravimetric analysis (TGA) that the complex began to lose weight after a temperature of 140 ºC. This indicates that the complex does not contain water molecules, and at a temperature of (420 ºC) with a weight loss of approximately 50% results from the process of changing from solid to liquid or the beginning of ligand decomposition, which takes place in three steps, the first at (440 ºC) and the second at (460-480 ºC), the percentage of weight loss continued to increase until the temperature reached (540 ºC), and at a temperature of (560 ºC) the percentage of weight loss reached more than 80% (Figure 4). There is clear consistency and alignment between both gravimetric thermal analysis and differential thermal [41, 42].

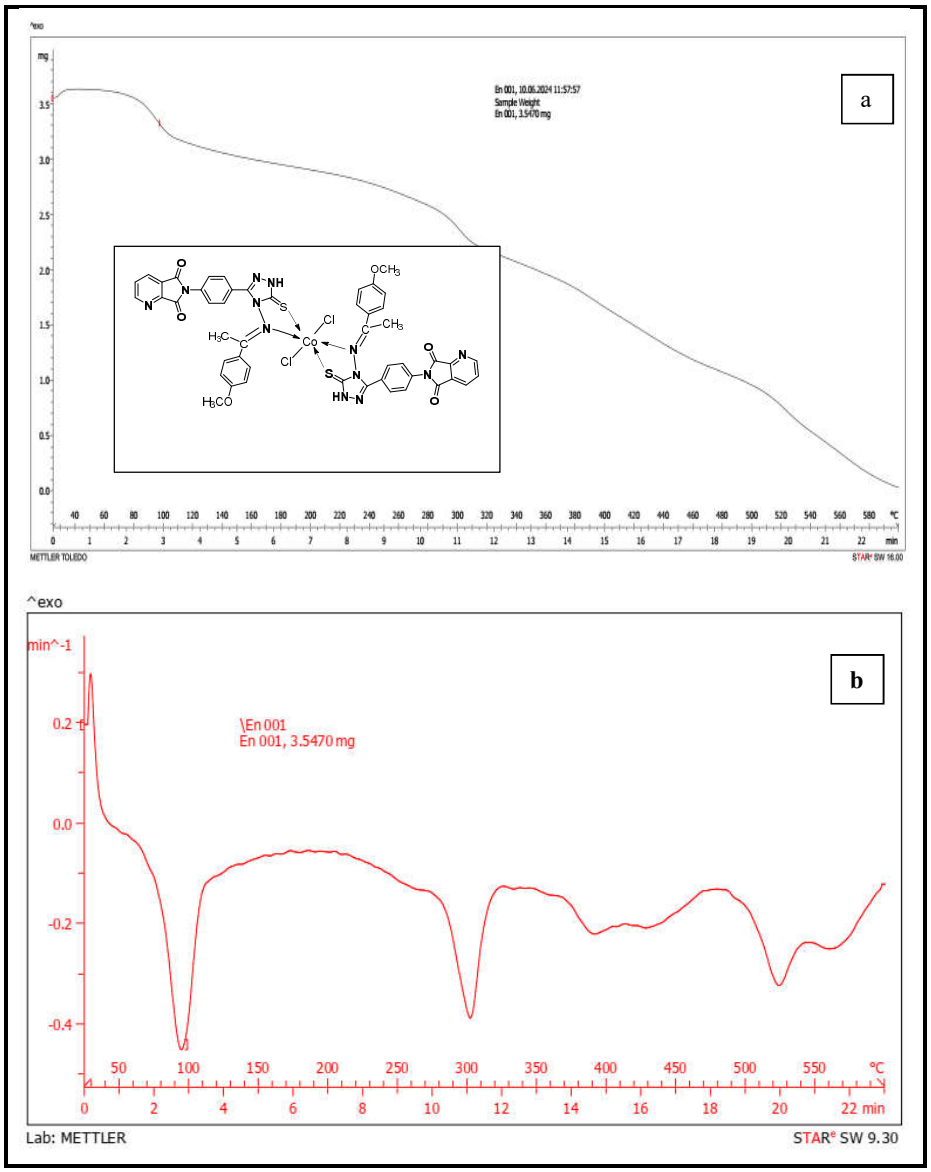

Figure 4. TGA (a) and DTA (b) $[Co(L_2)Cl_2]$ curves.

Biological activity

A number of generated compounds (L_1, L_2, **3**, **4**, **5**, **6**) had been evaluated for their biological effects against four different bacterial species, both Gram-positive and Gram-negative: *Staphylococcus aureus*, *Escherichia coli*, *Klebsiella pneumonia* and *Salmonella typhi*, Ampicillin

was also compared as a typical antibiotic. These bacteria were selected due to their significant role in the medical field—they cause a wide range of infections and show differing degrees of resistance to antibiotics and other medications. Table 2 displays the inhibitory results, which reveal that some of the prepared compounds demonstrated the ability to inhibit the growth of the tested bacteria. The inhibitory activity in Table reveals that (**4** and **6**) exhibited high effectiveness compared to free ligands against the tested bacteria [43, 44]. Figure 5 shows the inhibition zones of tested compounds.

Table 2. Biological properties of tested compounds.

Comp No.	*Staphylococcus aureus* (10 mg/mL)	*Escherichia coli* (10 mg/mL)	*Klebsiella pneumonia* (10 mg/mL)	*Salmonella typhi* (10 mg/mL)
L_1	12	13	16	14
L_2	13	15	12	14
$[Zn(L_1)Cl_2]$ (**3**)	15	15	13	15
$[Co(L_1)Cl_2]$ (**4**)	14	17	18	18
$[Co(L_2)Cl_2]$ (**5**)	13	15	----	16
$[Zn(L_2)Cl_2]$ (**6**)	17	16	17	17
Tetracycline (C1)	30	25	25	20

Inhibition levels are categorized as follows levels between 1 and 6 mm are classified as low inhibition; those ranging from 6 to 12 mm indicate moderate inhibition; and levels exceeding 12 mm are indicative of high impact and inhibition zone.

Molecular docking studies

Docking was carried out on a molecular target, which is the penicillin-binding protein of *Staphylococcus aureus,* which was downloaded from the protein data bank available at https://www.rcsb.org/structure/3VSK designated PDB ID:3VSK using the on-line server CB-dock2 [45] which can be accessed via https://cadd.labshare.cn/cb-dock2/php/index.php. The control was Pencillin G (PDB ID: PNM) according to method [44]. Interactions were visualized using the LigPlot tool [46]. Table 3 shows the docking scores of the synthesized compounds with their interactions as hydrogen bonds and hydrophobic interactions and share the same residue of Penicillin G, Arg504. Figure 7.

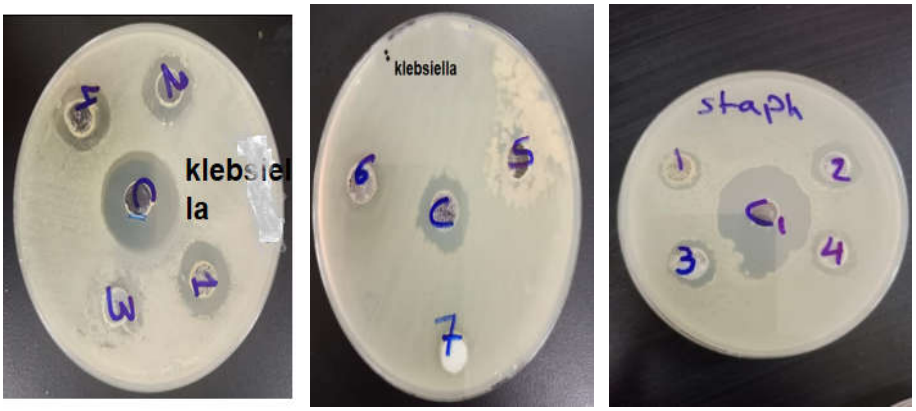

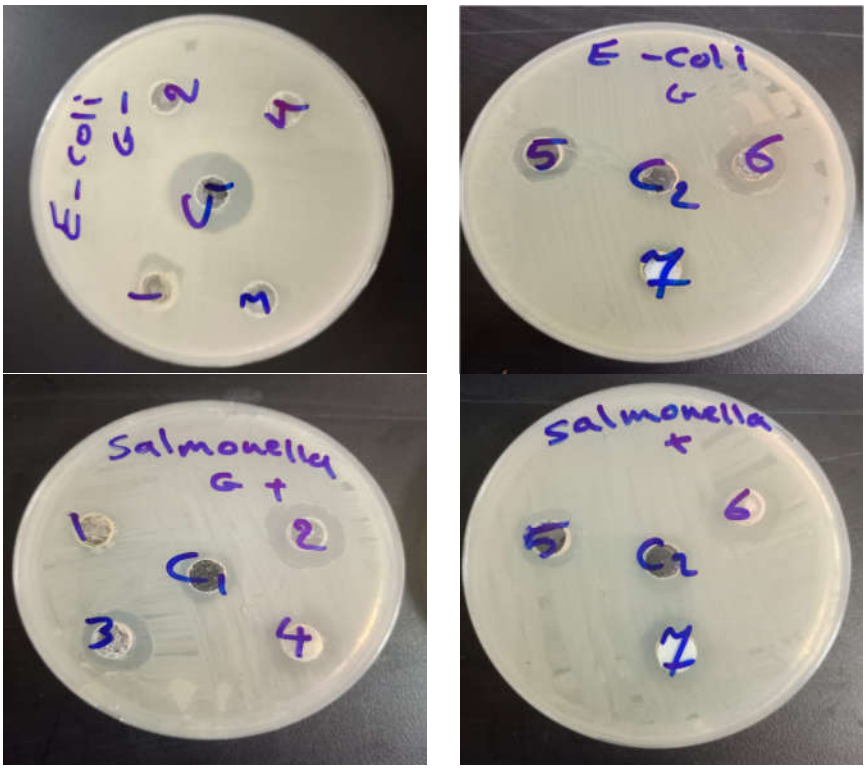

Figure 5. Inhibition zones (mm) of complexes with ligands for four types of bacteria.

Due to increasing antimicrobial resistance, scientists began to look for new alternative targets for antimicrobial action, such as the isoprenoid biosynthetic pathway, the shikimate synthesis pathway, plasmid partition systems, and the cytoskeleton, so these elements can be exploited by screening chemical compounds or natural products that inhibit enzymes essential for bacterial metabolism [47, 48]. Studied several molecular targets in bacteria using compounds of mushrooms as possible antibacterial agents, including penicillin-binding protein. Docking was performed using pencillin binding protein against compounds extracted from germainum kaempferol. germacrene A and elatine had binding affinities of -7.9, -7.1, and elatine -9.2 kcal/mol, respectively [49].

Table 3. Docking scores and interactions of the compound L_2.

Compound	Docking score	Hydrogen bonding	Hydrophobic Interactions
PNM	-7.8	Arg546,Lys494	Gly496,Thr495,Pro500,Tyr 278, Lys273,Asn501,Leu256,Glu255,Val493, His259,Leu576
L_2	-9.6	Arg504,Asn501,Arg546	Lys273,Tyr278,Pro500,Leu576, Leu256,His259,Glu258,Glu255

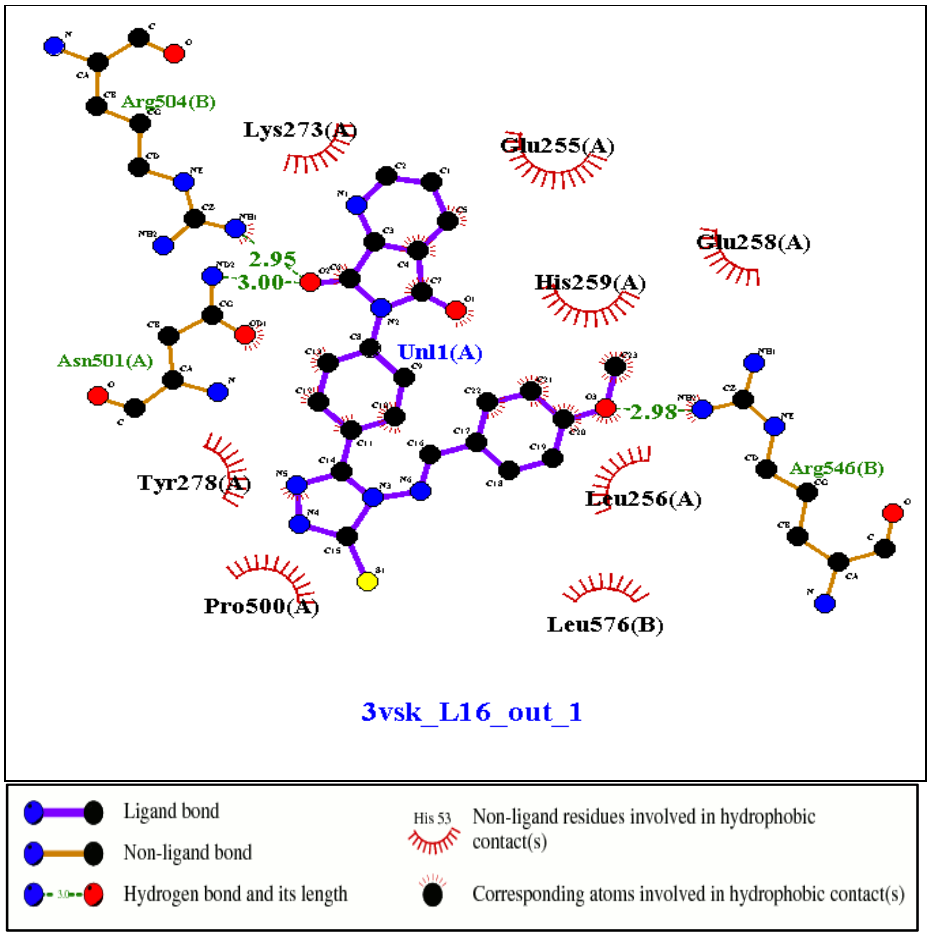

Figure 6. Interaction of L_2 with the molecular target 3VSK.

Structure for prepared compounds

According to the results discussed in our paper, compounds can be illustrated as shown in Figure 7.

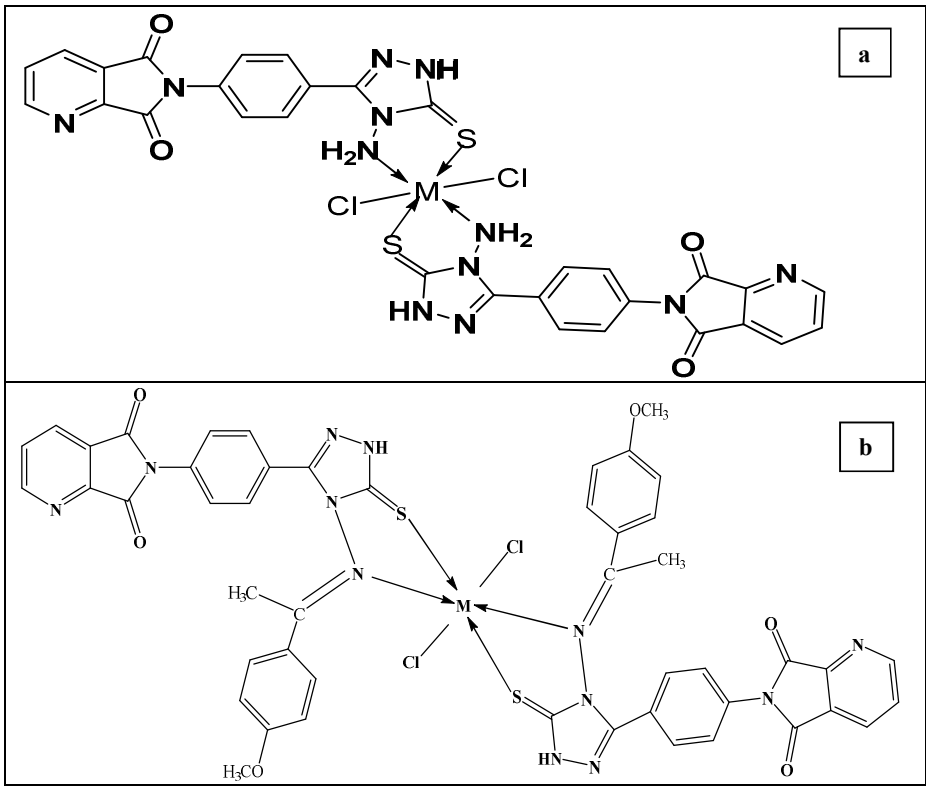

Figure 7. Proposed structure of synthesized complexes a **7-9**, b **10-12**. M = Co(II), Ni(II), Zn(II).

CONCLUSIONS

In this research we have successfully synthesized substituted membered heterocyclic compounds. These ligand compounds are converted to cobalt, nickel, and zinc complexes. From the various physical and spectroscopic studies mentioned earlier, the following conclusions can be drawn: Firstly, the ligands prepared for cobalt chloride, nickel chloride, and zinc chloride complexes exhibit identical ligand behavior. L_1 coordinate through nitrogen atom of amine group and sulfur atom of thiol group of L_1. As for the Schiff base ligand L_2, they coordinate with cobalt(II), nickel(II) and zinc(II) in a bi-dentate manner through the nitrogen atom of azomethine group and the sulfur atom of thiol group. Secondly, from the results of magnetic measurements and spectroscopic studies conducted on the prepared complexes, it can be inferred that they exhibit octahedral geometries. The biological study of some compounds revealed that a number of compounds have excellent inhibition against the bacteria, while others showed moderate to weak activity.

ACKNOWLEDGEMENTS

Our thanks are directed to the College of Education for Pure Sciences at Mosul University for helping to make the resources needed for this study available. Their cooperation was crucial to the successful completion of the research.

REFERENCES

1. Ju, F.Y.; Li, G.L.; Li, X.L.; Yin W.D.; Liu, G.Z. Syntheses, structures, and properties of twoCd(II)/Zn(II) complexes with 1,2,4-triazolederivatives. *Russ. J. Coord. Chem.* **2019**, 45, 600-607.
2. Liu, K.; Shi, W.; Cheng, P. The coordination chemistry of Zn(II), Cd(II) and Hg(II) complexes with 1,2,4-triazole derivatives. *Dalton Trans.* **2011**, 40, 8475-8490.
3. Kargar, H.; Torabi, V.; Akbari, A.; Behjatmanesh-Ardakani, R.; Sahraei, A.; Tahir, M.N. Pd(II) and Ni(II) complexes containing an asymmetric Schiff base ligand: Synthesis, X-ray crystal structure, spectroscopic investigations and computational studies. *J. Mol. Struct.* **2020**, 1205, 127642.
4. Adachi, J.; Mori, T.; Inoue, R.; Naito, M.; Le, N.H.T.; Kawamorita, S.; Hill, J.P.; Naota, T.; Ariga, K. Emission control by molecular manipulation of double-paddled binuclear Pt(II) complexes at the air-water interface. *Chem. Asian J.* **2020**, 15, 406-414.
5. Yang, G.H.; Li, Y.J.; Liu, D.; Cui, G.H. Dual-responsive luminescent sensor based on a water-stable Cd(II)-MOF for the highly selective and sensitive detection of acetyl acetone and Cr_2O_{72}−in aqueous solutions. *Cryst. Eng. Comm*. **2020**, 22, 1166-1175.
6. Tenorio, K.V.; Fortunato, A.B.; Moreira, J.M.; Roman, D.; De Oliveira, K.A.; Cuin, A.; Brasil, D.M.; Pinto, L.M.C.; Colman, T.A.D.; Carvalho, C.T. Thermal analysis combined with X-ray diffraction/Rietveld method, FT-IR and UV-Vis spectroscopy: Structural characterization of the lanthanum and cerium(III) poly crystalline complexes, *Thermochim. Acta* **2020**, 690, 178662.
7. Djunaidi, M.C.; Pardoyo, P.; Widodo, D.S.; Lusiana, R.A.; Yuliani, A. *In-situ* ionic imprinted membrane (IIM) synthesis based on acetic polyeugenoxy acetyltiophen methanolate for gold(III) metal ion transports. *Indones. J. Chem.* **2020**, 20, 1323-1331.
8. Omar, S.A.E.; Scattergood, P.A.; McKenzie, L.K.; Bryant, H.E.; Weinstein, J.A.; Elliott, P.I.P.Towards water soluble mitochondria targeting theranostic osmium(II) triazole-based complexes, *Mol*. **2016**, 21, 1382.
9. Bisceglie, F.; Bacci, C.; Vismarra, A.; Barilli, E.; Pioli, M.; Orsoni, N.; Pelosi, G., Antibacterial activity of metal complexes based on cinnamaldehyde thiosemicarbazone analogues. *J. Inorg. Biochem.* **2020**, 203, 110888.
10. Shukla, S.N.; Gaur, P.; Raidas, M.L.; Bagri, S.S. Synthesis, spectroscopic characterization, DFT, oxygen binding, antioxidant activity on Fe(III), Co(II) and Ni(II) complexes with a tetradentate ONNO donor Schiff base ligand. *J. Serb. Chem. Soc.* **2021**, 86, 941-954.
11. Rasyda, Y.A.; Widowati, M.K.; Marliyana, S.D.; Rahardjo, S.B. Synthesis, characterization and antibacterial properties of nickel(II) complex with 4-aminoantipyrine ligand. *Indones. J. Chem.* **2021**, 21, 391-399.
12. Idrees, M.; Nasare, R.D.; Siddiqui, N.J. Synthesis of S-phenacylated trisubstituted 1,2,4-triazole incorporated with 5-(benzofuran-2-yl)-1-phenyl-1*H*-pyrazol-3-yl moiety and their antibacterial screening. *Chem. Sin.* **2016**, 7, 28-35.
13. Ozadal, K.; Ozkanli, F.; Jain, S.; Rao, P.P.N.; Velazquez-Martinez, C.A. Synthesis and biological evaluation of isoxazolo[4,5-*d*]pyridazin-4-(5*H*)-one analogues as potent anti-inflammatory agents. *Bioorg. Med. Chem.* **2012**, 20, 2912-2922.
14. Kanagarajan, V.; Thanusu, J.; Gopalakrishnan, M. Synthesis and in vitro microbiological evaluation of novel 2,4-diaryl-3-azabicyclo[3.3.1]nonan-9,5′-spiro-1′,2′,4′-triazolidine-3′-thiones. *Med. Chem. Res.* **2012**, 21, 3965-3972.
15. Bharty, M.K.; Bharti, A.; Chaurasia, R.; Chaudhari, U.K.; Kushawaha, S.K.; Sonkar, P.K.; Ganesan, V.; Butcher, R.J. Synthesis and characterization of Mn(II) complexes of 4-phenyl(phenyl-acetyl)-3-thiosemicarbazide, 4-amino-5-phenyl-1,2,4-triazole-3-thiolate, and their application toward selector chemical oxygen reduction reaction. *Polyhedron* **2019**, 173, 114125.

16. Bhale, S.P.; Yadav, A.R.; Pathare, P.G.; Tekale, S.U.; Franguelli, F.P.; Kotai, L.; Pawar, R.P. Synthesis, characterization and antimicrobial activity of transition metal complexes of 4-[(2-hydroxy-4-methoxyphenyl) methyleneamino]-2,4-dihydro-3*H*-1,2,4-triazole-3-thione. *Eur. Chem. Bull.* **2020**, 9, 430-435.
17. Fathi, A.A.; Jawaheri, Y.S. Synthesis and characterization of new N- Aryl sulfonyl hydrazone compounds. *Egypt. J. Chem*. **2022**, 65, 179-183.
18. Devkota, K.; Pathak, G.; Shakya, G. Synthesis and evaluation of Schiff bases of 4-amino-5-(chlorine substituted phenyl)-4*H*-1,2,4-triazole-3-thione as antimicrobial agents. *J. Nepal Chem. Soc*. **2020,** 41, 26-35.
19. Abdelbaset, M.; Zabin, S.A. Vanadium(V) complexes containing 1,2,4-triazole moiety and their antimicrobial activity. *Int. J. Adv. Res.* **2016**, 4, 1861-1871
20. Murti, Y.; Agnihotri, R.; Pathak, D. Synthesis, characterization and pharmacological screening of some substituted 1,2,3- and 1,2,4-triazoles. *Am. J. Chem*. **2011**, 1, 42-46.
21. Jawad, W.A.; Balakit, A.A.; Al-Jibouri, M.N.A. Synthesis, characterization and antibacterial activity study of cobalt(II), nickel(II), copper(II), palladium(II), cadmium(II) and platinum(IV) complexes with 4-amino-5-(3,4,5-trimethoxyphenyl)-4*h*-1,2,4-triazole-3-thione. *Indones. J. Chem.* **2021***,* 21, 1514-1525.
22. Leven, M.; Berghe, V.; Mertens, F.; Vlietinck, A.; Lammens, E. Screening of higher plants for biological activities. Antimicrobial activity. *Planta Med.* **1979**, 36, 311-321.
23. Vandepitte, J.; Verhaegen, J.; Engbaek, K.; Piot, P.; Heuck, C.; Rohner, P.H.C.C.C. *Basic Laboratory Procedures in Clinical bacteriology*, World Health Organization: Gewneva; **1991**; 1, 121.
24. Haddad, R.; Yousif, E.; Ahmed, A. Synthesis and characterization of transition metal complexes of 4-amino-5-pyridyl-4H-1,2,4-triazole-3-thiol. *SpringerPlus* **2013**, 2, 1-7.
25. Narayana, B.; Gajendragad, M. Complexes of Zn(II), Pd(II), Hg(II), Pb(II), Cu(I), Ag(I), and Ti(I) with 4-amino-5-merccapto-3-(o-tolyloxymethyl)-1,2,4-troazol. *Turk. J. Chem*. **1997**, 21, 71-76.
26. Al-Assafe, A.Y.; Al-Quaba, R.A.S. Synthesis, characterization and antibacterial studies of ciprofloxaci-imines and their complexes with oxozirconium(IV), dioxomolybdenum(VI), and dioxotungsten(VI). *Bull. Chem. Soc. Ethiop*. **2024**, 38, 949-962.
27. Flifel, I.; Kadhim, S. Synthesis and chracterization of 1,3,4-oxadiazole derivatives with some new transition metal complexes. *J. Kerbalauni.* **2012**, 10, 197-209.
28. Bader, A.T.; Al-qasii, N.A.R.; Shntaif, A.H.; El Marouani, M.; Al Majidi, M.I.H.; Trif, L.; Boulhaoua, M. Synthesis, structural analysis and thermal behavior of new 1,2,4-triazole derivative and its transition metal complexes. *Indones. J. Chem.* **2022**, 22, 223-232.
29. Husain, A.Z.; Al-Jawaheri, Y.S.; Al-Assafe, A.Y. Synthesis of substituted heterocyclic with their cobalt(II)complexes from 2-aminothiazoles and evaluation of their biological activity, *Bull. Chem. Soc. Ethiop*. **2024**, 38, 909-922.
30. Jawad, W.A.; Al-Hussein Balakit, A.A.; Al-Jibo, M.N.A. Synthesis, characterization and antibacterial activity study of cobalt(II), nickel(II),copper(II), palladium(II), cadmium(II) and platinum(IV) complexes with 4-Amino-5-(3,4,5-trimethoxyphenyl)-4*H*-1,2,4-triazole-3-thione. *Indones. J. Chem.* **2021**, 21, 1514-1525.
31. Al-Jibouri, M.N.; Jawadb, W.A.; Balakitc, A.A.; Obies, M. Synthesis, characterization (theoretical and biological study) of some transition metal complexes with new Schiff base derived from 1,2,4-triazole. *Egypt. J. Chem.* **2021**, 64, 27-52.
32. Hamil, A.; Khalifa, K.M.; Almutaleb, A.A.; Nouradean, M.Q. Synthesis, characterization and antibacterial activity studies of some transition metal chelates of Mn(II), Ni(II) and Cu(II) with Schiff base derived from diacetylmonoxime with O-phenylenediamine. *Adv. J. Chem.* **2020**, 3, 524-533.

33. Amer, S.; El-Wakiel, N.; El-Ghamry, H. Synthesis, spectral, antitumor and antimicrobial studies on Cu(II) complexes of purine and triazole Schiff base derivatives. *J. Mol. Struct.* **2013**, 1049, 326-335.
34. Silverstein, R.; Webster, F.X.; Kiemle, D. *Spectrometric Identification of Organic Compounds*, 7th ed., John Wiley & Sons, Inc.: Hoboken, New Jersey, USA; **2005**.
35. Al-Assafe, A.Y.; Al-Quaba, R.A.S. Synthesis, characterization, and antibacterial studies of some of first transition series metals and zinc complexes with mixed ligands of trimethoprim-isatin and nitrogen base. *Bull. Chem. Soc. Ethiop*. **2024**, 38, 1013-1025.
36. Husain, A.Z.; Al-Jawaheri, Y.S.; Al-Assafe, A.Y. Synthesis of substituted 2-amino oxazoles with their cobalt(II) and platinum(IV) complexes and evaluation of their biologicalactivity. *Bull. Chem. Soc. Ethiop*. **2024**, 38, 1667-1679.
37. Al-Quaba, R.A.S.; Hasan, E.A.; Al-Assafe, A.Y. Synthesis and characterization of some transition metalcomplexes with Schiff base derived from 2,6-diaminopyridine. *Bull. Chem. Soc. Ethiop*. **2024**, 38, 1337-1350.
38. Al-Assafe A.Y.; Al-Quaba, R.A.S. New series of Ni(II), Cu(II), Zr(IV), Ag(I), and Cd(II) complexes of trimethoprim and diamine ligands: Synthesis, characterization, and biological studies. *Indones. J. Chem.* **2024**, 24, 812-821.
39. Al-Dobony, B.S.; Al-Assafe, A.Y. Synthesis, characterization and antimicrobial studies of some metal complexes with mixed ligands derived from Mannich bases and diamine ligands, *IOP Conf. Series: Journal of Physics: Conf. Series* **2019**, 1294, 1-11.
40. Abd El-Lateef, H.M.; Ali, A.M.; Khalaf, M.M.; Abdou, A. New iron(III), cobalt(II), nickel(II), copper(II), zinc(II) mixed-ligand complex: Syntheses, structural, DFT, molecular docking and antimicrobial analysis. *Bull. Chem. Soc. Ethiop.* **2024**, 38, 147-166
41. Al-Khazraji, A.M.A.; Al Hassani, R.M.A. Synthesis, characterization and spectroscopic study of new metal complexes form heterocyclic compounds for photo stability study. *Sys. Rev. Pharm.* **2020**, 11, 535-555.
42. AL-Jaffer, T.; Naser, Z.; Hameed, A. Spectroscopic and thermal studies of some palladium(II) complexes with 2-amino-4-(4-subsistuted phenyl) thiazole derivatives. *Biomed. Chem. Sci*. **2022**, 1, 78-82
43. Hany, M.A.E.; Ali, M.A.; Mai, M.K.; Aly, A. New Fe(III), Co(Π), Ni(Π), Cu(Π), and Zn(Π) mixed ligand complexes: Structural, DFT, biological, and molecular docking studies. *Bull. Chem. Soc. Ethiop*. **2024**, 38, 397-416.
44. Mohammed, F.A.; Al-barwari, A.S.M. Divalent transition metal complexes with mixed of β-enaminone and N,O-donor ligands: synthesis, characterization and biological assessment. *Bull. Chem. Soc. Ethiop*. **2025**, 39, 65-78.
45. Yang, L.; Xiaocong Y.; Jianhong G.; Shuang, C.; Zhi-Xiong, X.; Yang, C. Dock, C.B.: Improved protein–ligand blind docking by integrating cavity detection, docking and homologous template fitting. *Nucl. Acid. Res.* **2022**, 50, W159-W164.
46. Laskowski, R.A.; Swindells, M.B. LigPlot+: Multiple ligand-protein interaction diagrams for drug discovery. *J. Chem. Inf. Model*. **2011**, 51, 2778-2786.
47. Alves, M.J.; Froufe, H.J.; Costa, A.F.; Santos, A.F.; Oliveira, L.G.; Osório, S.R.; Abreu, R.M.; Pintado, M.; Ferreira, I.C. Docking studies in target proteins involved in antibacterial action mechanisms: Extending the knowledge on standard antibiotics to antimicrobial mushroom compounds. *Mol*. **2014**, 19, 1672-84.
48. Mir, W.R.; Bhat, B.A.; Rather, M.A. Molecular docking analysis and evaluation of the antimicrobial properties of the constituents of *Geranium wallichianum* D. Don ex Sweet from Kashmir Himalaya. *Sci. Rep*. **2022**, 12, 12547.
49. Al-Khayyat, M.Z. Molecular targets to develop future antimicrobials. *Bio. Technologia* **2019**, 10, 169-178.